LOAN DOCUMENT

DTIC ACCESSION NUMBER

LEVEL

INVENTORY

○

AFRL-ML-TY-TP-2002-4537

DOCUMENT IDENTIFICATION

21 May 2002

DISTRIBUTION STATEMENT A
Approved for Public Release
Distribution Unlimited

DISTRIBUTION STATEMENT

H
A
N
D
L
E

W
I
T
H

C
A
R
E

ACCESSION FOR

NTIS	GRA&I ☑
DTIC	TRAC ☐
UNANNOUNCED	☐
JUSTIFICATION	

BY

DISTRIBUTION/

AVAILABILITY CODES

DISTRIBUTION	AVAILABILITY AND/OR SPECIAL
A-1	

DISTRIBUTION STAMP

DATE ACCESSIONED

DATE RETURNED

20020807 228

DATE RECEIVED IN DTIC

REGISTERED OR CERTIFIED NUMBER

DTIC FORM 70A
JUN 90

DOCUMENT PROCESSING SHEET

PREVIOUS EDITIONS MAY BE USED UNTIL
STOCK IS EXHAUSTED.

LOAN DOCUMENT

AFRL-ML-TY-TP-2002-4537

Mass Transfer Effects on Kinetics of Dibromoethane Reduction by Zero-Valent Iron in Packed-Bed Reactors

Loraine, Gregory; Burris, David; Li Lixiong; and Schoolfield, John

Applied Research Associates, Inc.
215 Harrison Avenue
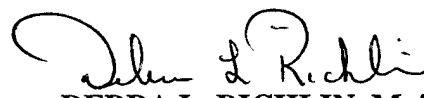Panama City, FL 32401

AQM02 - 11 - 2627

NOTICES

USING GOVERNMENT DRAWINGS, SPECIFICATIONS, OR OTHER DATA INCLUDED IN THIS DOCUMENT FOR ANY PURPOSE OTHER THAN GOVERNMENT PROCUREMENT DOES NOT IN ANY WAY OBLIGATE THE US GOVERNMENT. THE FACT THAT THE GOVERNMENT FORMULATED OR SUPPLIED THE DRAWINGS, SPECIFICATIONS, OR OTHER DATA DOES NOT LICENSE THE HOLDER OR ANY OTHER PERSON OR CORPORATION; OR CONVEY ANY RIGHTS OR PERMISSION TO MANUFACTURE, USE, OR SELL ANY PATENTED INVENTION THAT MAY RELATE TO THEM.

THIS TECHNICAL REPORT HAS BEEN REVIEWED AND IS APPROVED FOR PUBLICATION

ARTICLE REPRINT AVAILABLE FROM THE JOURNAL OF ENVIRONMENTAL ENGINEERING, VOL. 128, NO# 1, January 1, 2002, pp: 85-93

LARRY N. COOK JR., Capt, USAF
Program Manager

DEBRA L. RICHLIN, Maj, USAF
Deputy Chief, Weapons Systems Logistics
Branch

DONALD R. HUCKLE JR., Col, USAF
Chief, Air Expeditionary Forces Technologies Division

REPORT DOCUMENTATION PAGE

Form Approved
OMB No. 0704-0188

Public reporting burden for this collection of information is estimated to average 1 hour per response, including the time for reviewing instructions, searching existing data sources, gathering and maintaining the data needed, and completing and reviewing this collection of information. Send comments regarding this burden estimate or any other aspect of this collection of information, including suggestions for reducing this burden to Department of Defense, Washington Headquarters Services, Directorate for Information Operations and Reports (0704-0188), 1215 Jefferson Davis Highway, Suite 1204, Arlington, VA 22202-4302. Respondents should be aware that notwithstanding any other provision of law, no person shall be subject to any penalty for failing to comply with a collection of information if it does not display a currently valid OMB control number. **PLEASE DO NOT RETURN YOUR FORM TO THE ABOVE ADDRESS.**

1. REPORT DATE (DD-MM-YYYY) 21-05-2002	2. REPORT TYPE Final	3. DATES COVERED (From - To)

4. TITLE AND SUBTITLE
Mass Transfer Effects on Kinetics of Dibromoethane Reduction by Zero-Valent Iron in Packed-Bed Reactors

5a. CONTRACT NUMBER
F08637-98-C-6002

5b. GRANT NUMBER

5c. PROGRAM ELEMENT NUMBER

6. AUTHOR(S)
Loraine, Gregory; Burris, David; Li Lixiong; and Schoolfield, John

5d. PROJECT NUMBER
RAFCE80G

5e. TASK NUMBER

5f. WORK UNIT NUMBER

7. PERFORMING ORGANIZATION NAME(S) AND ADDRESS(ES)
ARA, Inc.

8. PERFORMING ORGANIZATION REPORT NUMBER

9. SPONSORING / MONITORING AGENCY NAME(S) AND ADDRESS(ES)
US Air Force Research Laboratory
139 Barnes Drive, Suite 2
Tyndall AFB, FL 32403-5323

10. SPONSOR/MONITOR'S ACRONYM(S)
AFRL-ML-TY-TP-02-4537

11. SPONSOR/MONITOR'S REPORT NUMBER(S)

12. DISTRIBUTION / AVAILABILITY STATEMENT
Approved for public release, distribution unlimited

13. SUPPLEMENTARY NOTES

14. ABSTRACT
"Mass transfer effects on the kinetics of 1,2-dibromoethane (EDB) reduction by zero-valent iron (ZVI) in batch reactors, a laboratory scale packed-bed reactor, and a pilot scale packed-bed reactor are described. EDB was debrominated by ZVI to ethylene and bromide. EDB sorption to the cast iron surface was nonlinear and was described by a Langmuir equation. Laboratory scale column studies showed a nonlinear dependence of EDB removal on flow rate and initial EDB concentration. A nonequilibrium model of EDB sorption and reaction dependent on mass transfer was constructed using the laboratory scale data. The model was verified using data from a larger pilot scale packed-bed reactor that was used to remove EDB from contaminated groundwater. The data show two distinct removal processes, an initial rapid phase dominated by mass transfer followed by a slower phase where surface reactions dominated. The model successfully predicted the transition from mass transfer controlled surface reaction controlled conditions in the pilot scale data." (Journal of Environmental Engineering January 2002 p 85)

15. SUBJECT TERMS
ethylene dibromide, dibromoethane, reduction, mass transfer, kinetics

16. SECURITY CLASSIFICATION OF: UNCLASS			17. LIMITATION OF ABSTRACT	18. NUMBER OF PAGES	19a. NAME OF RESPONSIBLE PERSON Larry Cook
a. REPORT final	**b. ABSTRACT**	**c. THIS PAGE**			**19b. TELEPHONE NUMBER** (include area code) (850) 283-6111

Standard Form 298 (Rev. 8-98)
Prescribed by ANSI Std. Z39.18

Mass Transfer Effects on Kinetics of Dibromoethane Reduction by Zero-Valent Iron in Packed-Bed Reactors

Gregory A. Loraine[1]; David R. Burris[2]; Lixiong Li[3]; and John Schoolfield[4]

Abstract: Mass transfer effects on the kinetics of 1,2-dibromoethane (EDB) reduction by zero-valent iron (ZVI) in batch reactors, a laboratory scale packed-bed reactor, and a pilot scale packed-bed reactor are described. EDB was debrominated by ZVI to ethylene and bromide. EDB sorption to the cast iron surface was nonlinear and was described by a Langmuir equation. Laboratory scale column studies showed a nonlinear dependence of EDB removal on flow rate and initial EDB concentration. A nonequilibrium model of EDB sorption and reaction dependent on mass transfer was constructed using the laboratory scale data. The model was verified using data from a larger pilot scale packed-bed reactor that was used to remove EDB from contaminated groundwater. The data showed two distinct removal processes, an initial rapid phase dominated by mass transfer followed by a slower phase where surface reactions dominated. The model successfully predicted the transition from mass transfer controlled to surface reaction controlled conditions in the pilot scale data.

Introduction

1,2-Dibromoethane or ethylene dibromide (EDB) is a common groundwater and soil pollutant. EDB was formally used as an antiknock additive in leaded gasoline and aviation fuel. It was also used as a pesticide for citrus and grains until its use as a fumigant was banned by the U.S. Environmental Protection Agency (EPA) in 1984. Contaminated groundwater sites are usually associated with pesticide use or fuel spills. U.S. EPA has established a maximum contaminant level (MCL) of 50 parts per trillion (ppt) for EDB in drinking water, due to its toxicity and carcinogenicity. The State of Massachusetts has set a MCL of 20 ppt.

Zero valent zinc was first reported as a reducing agent in the dihalo-elimination of EDB in 1874 (Baciocchi 1983). More recently, Rajagopal and Burris (1999) found that when EDB in water was exposed to Fe^0 the only observed products were ethylene and bromide

$$BrH_2CCH_2Br + Fe^0 \rightarrow H_2CCH_2 + 2Br + Fe^2 \qquad (1)$$

Recently zero valent iron (ZVI) has been applied to the remediation of contaminated groundwater (Gillhiam and O'Hannesin 1994). A great deal of work has been done on the reduction of chlorinated organics, nitrogenous organics, and dissolved metals by ZVI (Matheson and Tratnyek 1994; Agrawal and Tratnyek 1996; Siantar et al. 1996; Hundal et al. 1997; Sayles et al. 1997; Shokes and Moller 1999). Permeable ZVI reactive barriers have been put in place in a number of locations (O'Hannesin and Gillham 1998; Puls et al. 1998; Gavasker et al. 1999). A permeable reactive barrier (PRB) is a subsurface media (catalyst, reactive surface, or biological system) of high porosity that intercepts a plume of contaminated groundwater in situ and removes the contaminant of interest. The reduction rates of chlorinated ethenes [e.g., trichloroethylene (TCE) and tetrachloroethylene (PCE)] with ZVI are relatively slow, however, ZVI based PRB's can be used because low groundwater flow rates provide sufficiently long residence times for complete dechlorination.

EDB reacts faster than many chlorinated ethylenes. In similar experiments (5g Fisher 40 mesh iron and 100 mL DI) the half life of EDB was found by Rajagopal and Burris (1999) to be 1.3 h, and the approximate half lives of 1,1,1-trichloroethane, TCE and PCE were 1.6, 24, and 120 h, respectively (Johnson et al. 1996; Campbell et al. 1997). The faster reaction kinetics of EDB reduction by ZVI would allow for shorter residence times, possibly expanding the engineered treatment options available for EDB contaminated groundwaters.

Most in situ applications of ZVI PRB's require excavation of aquifer material and replacement with iron filings, which have cost and logistical limitations. If a relatively short reaction zone is adequate for groundwater flow rates, the use of hydraulic fracturing to emplace the ZVI PRB (Hocking et al. 1998) may be feasible.

Above ground packed-bed ZVI reactors may accommodate the higher flow rates required for the more traditional pump-and-treat operations. In the above ground treatment system the iron could be more easily replaced as needed due to loss of reactivity or clogging. Additionally, the system could be relocated as necessary.

In this study, the kinetics and mass transfer characteristics of EDB reduction in laboratory and pilot scale ZVI packed-bed reactors were examined. A model incorporating reaction kinetics

[1]Research Chemist, Air Force Research Laboratory, Material and Manufacturing Command, Tyndall AFB, FL 32405.

[2]Research Chemist, Air Force Research Laboratory, Materials and Manufacturing Command, Tyndall AFB, FL 32405.

[3]Senior Engineer, Applied Research Associates Inc., Gulf Coast Divisions, Panama City, FL 32405.

[4]Project Manager, AFCEE-UNITEC. Massachusetts Military Reserve, MA 02542.

and mass transfer limitations was developed and used to analyze the results from the experimental systems. The feasibility of treating EDB contaminated groundwater using (1) an above ground treatment system, and (2) a narrow width in situ reactive wall (that could be emplaced by hydraulic fracturing or jetting) were evaluated using the model.

Materials and Methods

Chemicals

The cast iron (GX-27, Master Builders, Cleveland) was used as received. The cast iron filings were nonuniform flakes and cylinders with an average particle diameter d_p of 0.36 mm. The surface area (SA) measured using the nitrogen BET method (Micrometrics, Flowsorb 2300, Norcross, Ga.) was 0.79 m^2/g. The sand (Ottawa Sand) was water rinsed and oven dried.

Water used in the packed-bed reactor studies was groundwater contaminated with EDB collected from the FS-12 treatment site at the Massachusetts Military Reservation, Mass. (FS-12 MMR). The pH ranged from 6.3 to 7.3 and dissolved oxygen concentrations ranged from 6.3 to 8.7 mg/L. The influent water temperature varied seasonally from 10.2 to 12.0°C. On-going monitoring of the FS-12 site gave the following water quality parameters; total dissolved solids=46.4 mg/L, total suspended solids=2.3 mg/L, total organic carbon=0.33 mg/L, Fe=40.81 μg/L, Mn=16 μg/L, oxidation-reduction potential=260 mV.

Dibromoethane (Photrex grade) was obtained from J. T. Baker. Acetonitrile [high-pressure liquid chromatography (HPLC) grade], Methanol (HPLC grade), and p-dichlorobenzene (DCB, reagent grade) were obtained from Fisher Scientific. Pentane [trihalomethane (THM) grade] was obtained from Aldrich.

Batch

The batch kinetic experiments were conducted in 160 mL crimp top glass vials sealed with Teflon faced rubber septa, 100 mL of unbuffered de-ionized (DI) water, anaerobic headspace, and 5 g iron were spiked with 1–10 μL EDB (0.011–0.12 mM). The vials were rotated at 24 rpm (0.51 m/s) in the dark. Reaction temperatures were maintained in incubators, at 5, 10, 20, 30, and 40 (±1)°C. The mass balance experiments were performed at 20°C. Headspace samples (100 μL) were periodically obtained using a gas-tight syringe and analyzed by GC/FID. Control samples with no iron were run concurrently and showed negligible loss of EDB over several days. All experiments were run in duplicate.

Sorption experiments were run in zero headspace batch systems with duplicate, sacrificial samples. Iron filings (1.5 g) were placed in 15 mL serum vials, vials were filled completely with DI water (~14.8 mL) in an anaerobic chamber (H$_2$ 5%, N$_2$ 95%) and crimp sealed with Teflon faced rubber septa. Immediately after being sealed the vials were removed from the chamber and spiked with methanol solutions of dibromoethane (~1,260 mg/mL) to give a final concentration of ~85 mg/L (0.45 mM). The water volume of each vial was determined gravimetrically. Control samples contained no iron. The samples were mixed by axial rotation on a roller drum at 24 rpm, at 20±1°C in the dark. Duplicate control and experimental samples were removed after varying periods of time and analyzed to determine aqueous and total EDB concentrations. Duplicate 20 μL aliquots of the aqueous phase were sampled from each vial and spiked into 1.0 mL of acetonitrile with 10 mg/L p-dichlorobenzene as an internal standard and vortexed. Total system EDB concentrations were deter-
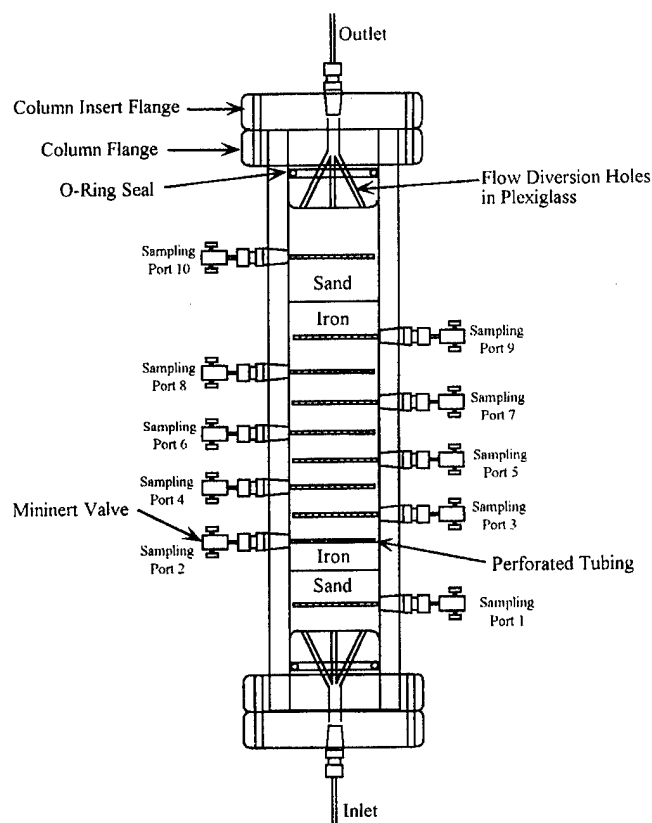

Fig. 1. Schematic of laboratory scale packed-bed reactor

mined by transferring the aqueous content of each vial into a 40 mL vial containing 10 mL of acetonitrile via cannule. The remaining solids were washed with two 2.5 mL portions of acetonitrile (spiked with internal standard) and the washing solvents added to the 40 mL vial. A 100 μL aliquot was spiked into 0.90 mL of acetonitrile and analyzed via GC/ECD.

The difference between the total and aqueous phase EDB masses was assumed to be the EDB mass bound to the metal surface. The sorption isotherm (20°C) was made by plotting the bound concentration (μg/m^2) versus the aqueous concentration (mol/m^3) as the reaction progressed.

Laboratory Scale Packed-Bed Reactor

The lab scale reactor (Fig. 1) was a column made of Plexiglas [19.7 cm length×2.54 cm inner diameter (i.d.)] with stainless steel sampling ports and fittings. Stainless steel screens were placed at the column inlet and outlet followed by 22 g sand, 254 g iron, and 28 g sand (inlet end down). Sampling ports 1 and 10 were located in the sand zones. Sampling ports 2–9 were located in the iron zone (12.7 cm in length). The sampling ports were 0.158 outer diameter×0.127 cm i.d. tubing with vertical half slots, attached to the column using 0.158×0.158 cm bore through male NPT Swagelok fittings with Teflon inserts to minimize dead volume. Mininert valves were placed on the end of sampling tube to facilitate sampling.

The pore volume was determined by pumping a known volume of water through the dry columns and collecting the effluent, the difference was taken to be the total column pore volume (186±3 mL). As H$_2$ was produced during operation of the iron column, pore water was displaced; thus the actual pore volume during operation was slightly less than that determined. The po-
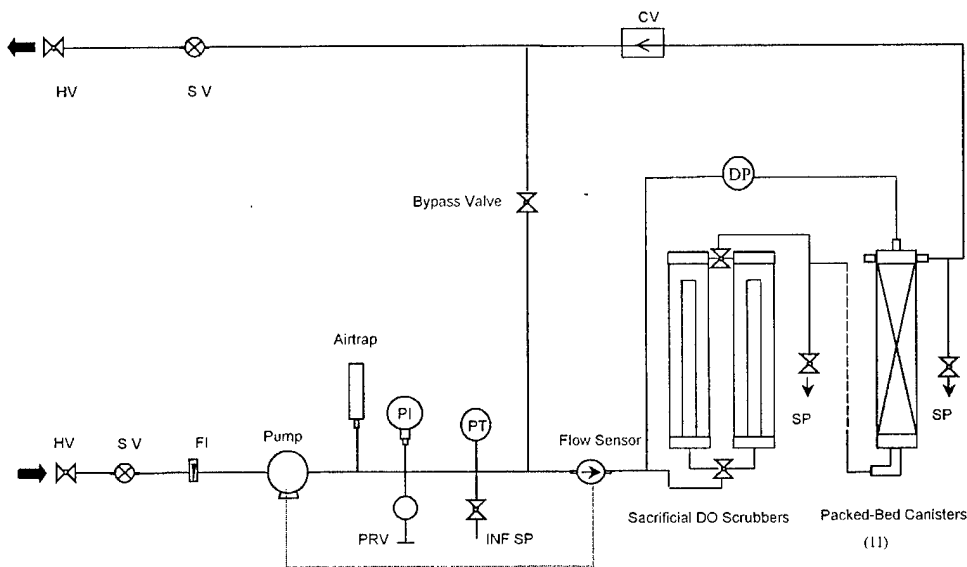
Fig. 2. Schematic of zero valent iron pilot scale packed-bed reactor. HV=hand valve, SV=solenoid valve, FI=Rotometer, Pump-variable speed pump, Airtrap=water hammer suppressor, PRV=pressure relief valve, PI=pressure gauge, PT=electronic pressure sensor, INF SP=influent sample port, Flow sensor, Sacrificial DO Scrubbers=one in-line, one in reserve, packed-bed canisters (11), SP=Sample ports (12), DP=differential pressure gauge, bypass valve, and CV=check valve.

rosity (ε) was found by dividing the pore volume by the empty bed volume of the column ($\varepsilon = 0.53 \pm 0.05$). This number includes the porosity in the sand layers, because of the relatively small amount of sand used, the error in the measured porosity was assumed to be small.

The column was sampled at various time intervals at sampling ports 1–10. Samples were drawn from the top sampling port first, sequentially to the influent. Samples were collected using a 150 μL syringe and the first 100 μL was discarded (dead volume ~25 μL). The 50 μL sample was then diluted as described below and analyzed by GC/ECD.

Flow was maintained with either an ISCO 2350 or Waters 510 (Waters, Milford Mass.) HPLC pump, at rates of 1.00 ± 0.05, 5.00 ± 0.25, and 10.0 ± 0.5 mL/min; flow rates were measured periodically through out the experiment to ensure consistency. The influent water was groundwater collected at FS-12 MMR, spiked with stock solutions of EDB in methanol (several microliters into 18 L of water). The influent water was stored in 18 L Teflon bags to prevent loss due to volatilization and covered with black plastic to prevent photolysis of EDB. Reduction rates of EDB in spiked site water and spiked DI water were identical.

The column required several pore volumes before the EDB profile reached steady state conditions. After steady state was reached (a minimum of 10 pore volumes) each sample port was sampled at least three times over several hours (tens of pore volumes). The flow rate was then increased and the system was allowed to reach steady state again before sampling was resumed.

Pilot Scale Packed-Bed Reactor

Fig. 2 shows a schematic of the pilot scale packed-bed reactor. The influent water, FS-12 groundwater, was taken from the 9 in. (22.9 cm) influent pipe at the existing treatment plant. The water was filtered through a stainless steel strainer (20×20 mesh). Two sets of shutoff valves controlled the influent and effluent flow, one manual the other a normally closed solenoid valve controlled by the process control system. A rotometer indicated flow into the system. Flow rate was controlled by a NEMO variable speed,

progressing cavity pump (Netzsch Inc., Exton, Penn). The pump speed was controlled with an AC Tech variable speed ac motor drive (AC Tech). The lower limit of the NEMO pump was 1,000 mL/min. In order to operate the system at lower flow rates a portion of the flow was shunted through a bypass. A manual valve controlled the volume of water bypassed.

The emergency solenoid cutoff valves, the pump and the instrumentation were controlled using a process control software package, *Lookout* (National Instruments, Austin, Tex.), an object-based automation software system. The software was resident on a Pentium PC with an I/O board, AT-M10-16E-10 (National Instruments, Austin, Tex.) and digital acquisition software, DAQ (National Instruments, Austin Tex.) A pressure transducer (maximum pressure 1,000 psi, accuracy$\pm$0.25%, Barksdale, Los Angeles), and a stainless steel pressure gauge (maximum pressure 300$\pm$5 psi, McMaster-Carr, Atlanta) were used to monitor and display influent pressure. The flow measured by the flow sensor (Flo-Sensor 102-7P, 100–2000 mL/min, $\pm$3% FS, McMillan Co., Georgetown Tex.) was read by the process control system and used to determine the pump speed; thus the flow rate remained constant against increasing backpressure. The flow was manually checked periodically. The pressure drop across the packed-bed reactor was measured by a differential pressure sensor-transmitter (Orange Research, Milford Conn). If the differential pressure exceeded 150 psi the pilot plant automatically shut off and an emergency pressure relief valve opened. *Lookout* automatically logged the influent pressure, differential pressure, flow through the flow transmitter, and the calculated flow through the bypass line.

The packed-bed reactor consisted of 12 stainless steel canisters (length=53.3 cm, diameter=8.9 cm, empty volume=3,316 cm^3, Osmonics, Minnetonka Minn.) plumbed in series with 0.95 cm stainless steel tubing and Swaglok fittings. All canisters were identical with the exception of the first. In the bottom of the canisters were stainless steel wire mesh screens (32×32 mesh) followed by a 2.5 cm deep layer of fine sand to distribute flow. The rest of the canister was filled with approximately 9.0 kg of cast iron filings. The exit of the canister was packed with stainless

steel wool to prevent washout. Samples were taken after each canister and at the influent prior to the flow sensor. A check valve after the last canister prevented backflow. The system effluent re-entered the 9 in. FS-12 treatment system influent pipe 61 cm downstream of the intake point.

The first canister was designed to remove DO with minimal increase in pressure drop. It had a 2.5 cm×38 cm stainless steel wire mesh (32×32 mesh size) center tube filled with fine sand, surrounded with cast iron to the top of the canister. The porosity of the sand was less than that of the iron filings, so preferential flow was through the iron. As the iron at the bottom oxidized and the permeability decreased, the water flowed up the center post and spread into the fresh iron. Thus as a portion of the iron was used up a new area was exposed. Two DO scrubbers were in parallel so a fresh canister could be put on line without interrupting the flow. Each canister was used until the pressure drop reached 100 psi, after that it was replaced. The useful lifetime depended on flow rate and influent DO. Canisters 2–12 were kept in service throughout the duration of the study. The DO in these canisters never exceeded 0.5 mg/L. Sampling was not performed for at least 24 h after switching to a new scrubber canister to allow the system to reach steady state.

Pilot plant samples were collected in 40 mL amber VOA vials. Canisters were sampled in reverse order, 12 to influent. Duplicate samples were taken at canister 6 and the influent. The vials were completely filled, without headspace, with no preservative. Samples were shipped overnight with icepacks and refrigerated until extraction. All samples were extracted as described below within 24 h of arriving at the laboratory.

Analytical

Headspace samples were collected and directly injected into a Hewlett-Packard 5890 GC equipped with a FID detector. The column was a DB-5 (30 m i.d. 0.53 mm, flow rate 3.5 mL/min); the oven program was isothermal at 40°C. Relative response factors were determined for EDB (dimensionless Henry's constant at 20°C was 0.035) and ethylene (H=8.9) (Sanders 1999), by adding known masses to 160 ml vials containing the same liquid/vapor ratio as the reaction vials. Standards were equilibrated at the same temperature as the reaction vials (Rajagopal and Burris 1999).

The method of sample extraction depended on the expected concentration. For EDB concentrations less than 20 ppb (pilot scale and low [EDB] lab scale samples), a 5 mL aliquot was transferred to an 8 mL test tube and ~0.50 g of NaCl was added. The tube was capped with a Teflon lined cap and mixed to dissolve the salt. The aliquot was extracted with 0.20 mL of THM grade pentane spiked with 5.0 μg/mL DCB as an internal standard, and shaken. The pentane layer was transferred to a 100 μL insert in a 2 mL crimp top vial for analysis. For samples of EDB>20 ppb (high [EDB] lab scale samples), a 50 μL sample was immediately spiked into autosampler vials containing 100 μL 10 ppm DCB as an internal standard in acetonitrile. At higher concentrations (10,000 ppb), a 50 μL aliquot was immediately diluted with 1 mL of acetonitrile containing 10 ppm DCB in a crimped GC vial.

Samples from the laboratory columns were analyzed for EDB on a Hewlett-Packard GC equipped with an electron capture detector (ECD). Samples were injected in splitless mode (split after 60 s) at 150°C onto a HP-1 column (3 μm thickness, 0.53 mm i.d., 15 m length). The oven temperature program was 40°C for 2 min and ramped at 20°C/min to 220°C. ECD temperature was
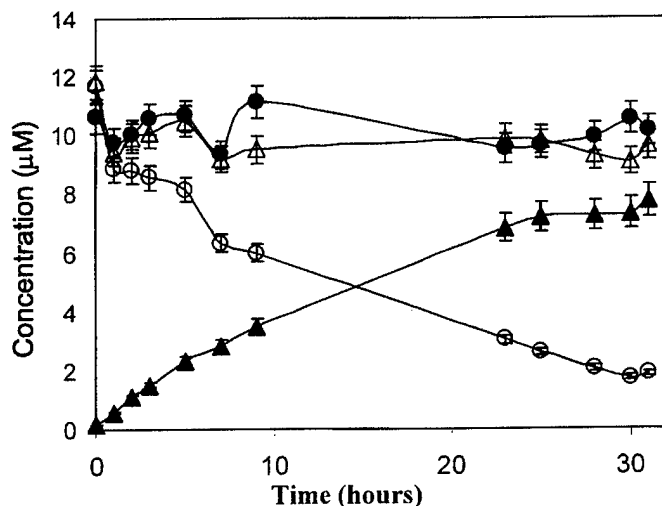

Fig. 3. Reduction of ethylene dibromide (EDB) by ZVI in a well-mixed system. [EDB]$_0$=11.8 μM, 5 g iron, 100 mL DI, headspace 60 mL. Vials were mixed at 24 rpm in the dark at 20°C. The only organic product found was ethylene. Control (no Fe^0) ($\bullet$), EDB ($\bigcirc$), C$_2$H$_4$ ($\blacktriangle$), C mass balance ($\triangle$).

280°C. Helium was the carrier gas (4.77 cm^3/min) and the detector make up gas was 5% methane in argon (57 cm^3/min). The EDB detection limit was 0.05 ppb.

Dissolved oxygen, pH, and temperature were measured in the field at the time of sample collection. Temperature and DO were measured using a YSI model 58 Dissolved Oxygen Meter with a YSI 5905 BOD probe (YSI Inc. Yellow Springs, Ohio). The DO meter was calibrated before each use to 100% air saturation. An Orion 250 A electrode was used for pH monitoring (Orion Research Inc., Boston).

Results and Discussion

Batch System

Results of a typical experiment in the batch system at 20°C are given in Fig. 3. The only organic product detected was ethylene and the carbon mass balance was near 100%. This is in agreement with Rajagopal and Burris (1999) who studied the reduction of EDB by Fisher 40-mesh cast iron. They determined that ethylene was the major product of EDB reduction and that no bromoethane or vinyl bromide was formed.

Pseudo-first-order rate constants relative to surface area (k_1) were determined at five temperatures (5, 10, 20, 30, and 40°C). k_1 at 20°C was found to be independent of initial EDB concentration (0.011–0.12 mM) and independent of mixing rate at rotation speeds greater than 8 rpm (data not shown). The portion of EDB in the headspace was less than 10% (Rajagopal and Burris 1999), thus the vapor-liquid partitioning was not expected to significantly affect the reaction kinetics. An Arrhenius plot [Eq. (10)] returned an Arrhenius parameter $A = 2.28 \times 10^8$ s^{-1} m^{-2} and an activation energy of $E_{a\,MB} = 55 \pm 13$ kJ/mol (Rajagopal and Burris found an $E_a = 51 \pm 7$ kJ/mol for Fisher 40-mesh cast iron).

The sorption isotherm for EDB was measured using relatively high concentrations of EDB and small amounts of metal so that the system had time to equilibrate and samples could be taken before a significant fraction of EDB was reacted (Fig. 4). The
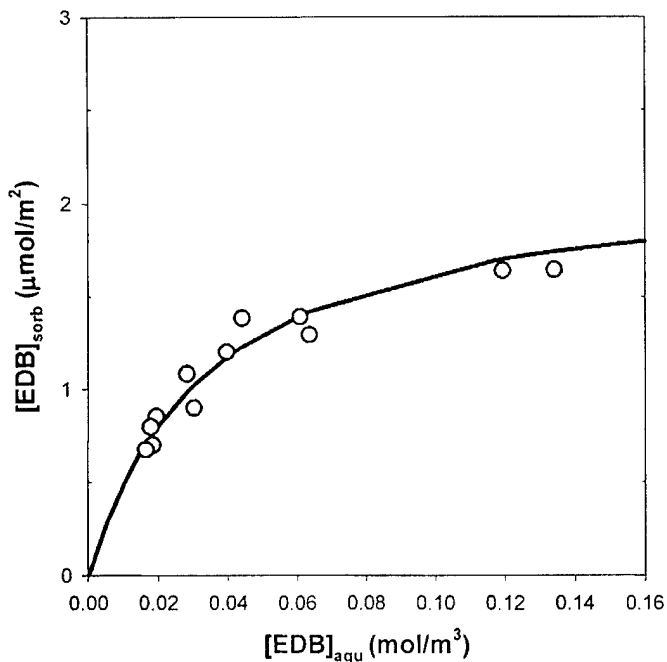
Fig. 4. Sorption isotherm of ethylene dibromide (EDB) on MB cast iron at 20°C. The line was fit using a Langmuir equation, $K_{ads} = 29.53$ and $EDB_{max} = 2.17 \times 10^{-6}$ mol/m^2.

Fig. 5. Observed removal rate constants (k_{obs}) of EDB in lab scale reactor at different flow rates 1, 5, and 10 mL/min, and initial concentrations, 6 (●), 100 (○), 1,000 (▼), 10,000 ppb (∇).

high EDB concentration also reduced possible interference by reaction products. The sorption isotherm was fit using the Langmuir equation [Eq. (4)] $EDB_{max} = 2.17 \times 10^{-6}$ mol/m^2 and $K_{ads} = 29.53$ m^3/mol. Burris et al. (1998) showed that sorption of halogenated organics to cast iron surfaces occurs at both reactive and nonreactive sorption sites. The relative concentration of reactive sites to nonreactive sites on the cast iron was not determined. The sorption isotherm in Fig. 4 was for sorption to all sites. In a well-mixed system mass transfer is rapid and steady state conditions are established quickly. It was assumed that the change in aqueous EDB concentration was due to reaction at active sites and sorption from the aqueous phase to the open active site.

Laboratory Scale Packed-Bed Reactor

Groundwater received from FS-12 MMR was filtered and spiked with EDB and used as influent solutions for the lab scale studies. Pseudo-first-order observed removal rate constants (k_{obs}) determined at different initial EDB concentrations and flow rates are shown in Fig. 5. The rate constants were calculated after steady state conditions were reached. At low initial EDB concentrations k_{obs} values increased when flow rate increased. At higher initial EDB concentrations k_{obs} values were lower and less dependent on flow rates. To understand the effects of concentration and flow rate on observed removal rates it is instructive to look at a conceptual model of heterogeneous reactions.

Model

A heterogeneous reaction can be thought of as a three step process, (1) adsorption-desorption of the substrate on the surface, (2) reaction of the surface bound substrate, and (3) the desorption of the products (Carberry 1976). Assuming steps 1 or 2 are rate limiting, the removal rate constant of an aqueous solute (k_{obs})
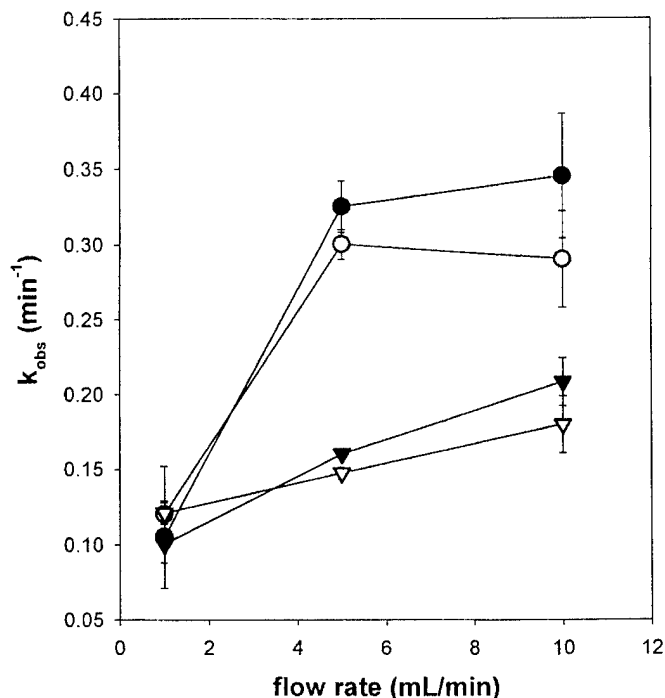
depends on mass transfer to and from the surface and the reaction rate on the surface (intraparticle diffusion was neglected).

$$k_{obs} = -k_{mt}a[C_{aq}] - k_1 a[C_{surf}] \qquad (2)$$

where k_{mt} (m^3/m^2 s) = rate constant of mass transfer, k_1 (m^3/m^2 s) = rate constant of the surface reaction, a = ratio of solid surface area to liquid volume (m^2/m^3), and C_{surf} (mol/m^2) = concentration of solute sorbed to the solid surface. When the rates of transfer to and from the sorption sites are equal the system is in equilibrium and the overall mass transfer is zero. Arnold et al. (1999) showed that mass transfer effects were greater for substrates with faster surface reaction rates. Since EDB reacted relatively rapidly mass transfer was expected to be more important than with slower reacting species. The k_{obs} for EDB at higher flow rates (5, 10 mL/min in Fig. 5) indicated that mass transfer did affect the kinetics and that this effect declined as aqueous concentration increased. In order to elucidate the mass transfer effects in packed-bed reactors, the aqueous EDB concentration profiles through the lab scale column at experimental flow rates and concentrations were simulated using a one dimensional nonequilibrium model.

Fig. 6 shows the aqueous EDB profiles through the lab scale reactor at two flow rates, 1 mL/min and 10 mL/min ([EDB]$_0$ = 6 ppb), and the lines that were fit to the data by the model described below. The model used values of C, S, and K_{in} of 1.15×10^{-4}, 0.69, and 12.7 (m^3/m^2), respectively. These values were determined by least squares regression using Powell's algorithm (Micromath). Average values of C, S, and K_{in} were calculated and used to simulate the data (solid lines in Fig. 6). The r^2 values of the model simulations of the experimental lab scale data were ≥ 0.93.

In systems with high liquid flow rates and surface reactions, partitioning equilibrium between liquid and solid phases may be retarded. The dependence of EDB removal in the lab scale col-
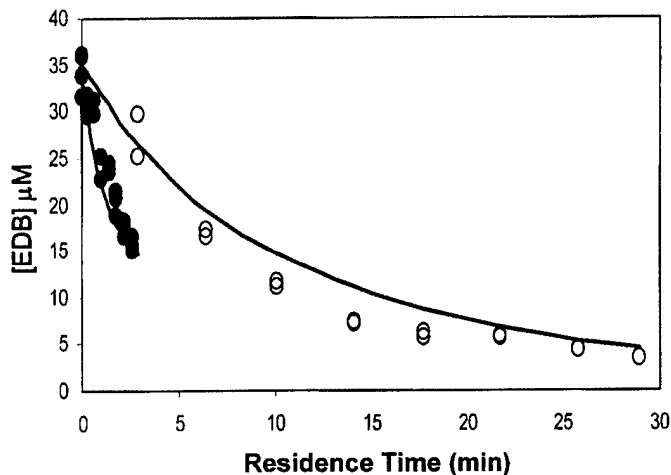
Fig. 6. Modeling of lab scale packed-bed reactor data at two flow rates 1 mL/min and 10 mL/min, using one-dimensional nonequilibrium model. The model parameters C, S, and K_{in} were determined by fitting the model to the data sets from the lab scale reactor. Duplicate data (O) are fit by the model (—). $[EDB]_0 = 6$ ppb, $C = 1.15 \times 10^{-4}$, $S = 0.69$, $K_{in} = 12.7$ m^3/m^2.

Table 1. Linear Velocities, Reynolds Numbers, and Reactor Length/Area Ratios (L/A) for Flow Rates in Bench Scale Column (1, 5, and 10 mL/min), Pilot Plant (300, 600, and 2,000 mL/min), and Hypothetical Full Scale Treatment System (2.3×10^6 mL/min)

Flow (mL/min)	V (m/s)	N_{Re}	L/A (m^{-1})
1	6.2×10^{-5}	0.025	3.9
5	3.1×10^{-4}	0.127	3.9
10	6.2×10^{-4}	0.250	3.9
300	1.5×10^{-3}	0.606	10.3
600	3.0×10^{-3}	1.21	10.3
2,000	1.0×10^{-2}	4.07	10.3
2,300,000	7.3×10^{-3}	3.0	8.3

Note: The model can be scaled up as long as the L/A and N_{Re} are within the same order of magnitude.

umn on aqueous solute concentration and flow rate indicated nonequilibrium conditions. Describing these nonequilibrium systems required a kinetic sorption model. A bilinear adsorption model is the kinetic version of the Langmuir isotherm (Fetter 1993).

$$\frac{d[EDB]}{dt} = -k_{forw}[EDB](S_{sat} - [EDB_{surf}]) + k_{rev}[EDB_{surf}]$$

(3)

Mass transfer to and from the solid surface controls the change in the aqueous concentration of EDB. k_{forw} is the rate of transfer to the surface and k_{rev} is the rate of transfer from the surface to the liquid, EDB_{surf} is the concentration of EDB on the surface and S_{sat} is the EDB_{surf} concentration at equilibrium. The S_{sat} can be found from the Langmuir sorption isotherm.

$$S_{sat} = \frac{EDB_{max} \times K_{ads}[EDB]}{1 + K_{ads}[EDB]}$$

(4)

where $EDB_{max} =$ maximum concentration of surface sites, (which is approached asymptotically as the aqueous concentration increases) and $K_{ads} =$ equilibrium constant found from the sorption isotherm (Fig. 4).

As $[EDB_{surf}]$ approaches the equilibrium surface concentration the first term on the right-hand side of Eq. (3) approaches zero and the rate of mass transfer declines. At higher aqueous phase concentrations the sorption sites on the surface were saturated. The effects of higher linear velocities on removal rates became weaker as the maximum EDB surface concentration was approached. Thus depending on the aqueous phase concentration the reaction was mass transfer limited, surface reaction limited or a combination of the two.

The second driver of mass transfer was the flow rate. The flow rate (m^3/s) was transformed to the linear velocity (V), which was the flow divided by cross-sectional area of the column (A), and porosity (ε).

$$V = \frac{f}{A\varepsilon}$$

(5)

The particle Reynolds number (N_{Re}) was dependent on the linear velocity (V), the average cross sectional diameter of the particles (d_p) and the kinematic viscosity of water (η)

$$N_{Re} = \frac{d_p V}{\eta}$$

(6)

The particle Reynolds numbers for flow rates used in this study are given in Table 1. These were very low Reynolds numbers and indicated a laminar flow regime.

Wilson and Geankopolis (1964) developed an empirical equation for mass transfer in packed-bed reactors. Starting from this equation the value of k_{forw} was estimated

$$k_{forw} = C \times N_{Re}^S \times Sc^{1/3} \times \frac{D_{EDB}}{dp}$$

(7)

where C and S are constants whose values were determined by performing a least squares regression of the column data for the two lowest EDB concentrations, 6 and 100 ppb, at three flow rates. Data from the laboratory scale reactor were modeled and the values of C and S were varied until the residual differences between the experimental EDB data and the predicted EDB concentrations reached a minimum. The 6 and 100 ppb data showed the greatest dependence on mass transfer so this data was used to fit C and S, obtaining 1.15×10^{-4} and 0.69, respectively.

D_{EDB} is the diffusivity of EDB in water at a specific temperature, and Sc is the Schmidt number. The Schmidt number is the diffusivity of a molecule in a given fluid.

$$Sc = \frac{\eta}{D_{EDB}}$$

(8)

k_{forw} is dependent on system parameters such as particle diameter and porosity, which were constant and variables dependent on temperature (Sc, η, D_{EDB}) and linear velocity (N_{Re}). In the lab scale studies the reaction temperatures (22–23°C) are higher than in the pilot scale system (9–12°C). The temperature dependence is included so the model could be applied to both sets of data.

When the surface concentrations were low $k_{forw}[EDB](S_{sat} - [EDB_{surf}]) > k_{rev}[EDB_{surf}]$. Under these nonequilibrium conditions the sorption of EDB to the surface was greater than desorption. This created transient conditions where mass transfer limitations were diminished and removal rates much higher than those observed at higher aqueous phase concentrations or lower linear velocities were achieved. Such transient conditions were described by Fetter (1993) for the sorption of inorganic solutes onto mineral surfaces. On reactive surfaces where surface solute con-

centrations were affected by a chemical process (k_1) and a physical process (k_{rev}) these transient conditions are maintained longer.

At equilibrium, $K_{ads} = k_{forw}/k_{rev}$. In the model, it was assumed that $k_{rev} = k_{forw}/K_{ads}$. Because the lab scale data inputted into the model was collected after the system reached steady state, it was necessary to estimate the concentration of EDB on the surface in the initial model parameters. The boundary conditions were $0 < [EDB_{surf}]_0 < S_{sat}$. k_{rev} was not a true constant as written, to account for this $[EDB_{surf}]_0$ was set to

$$[EDB_{surf}]_0 = \frac{EDB_{max}K_{in}[EDB]}{1 + K_{in}[EDB]} \quad (9)$$

where $K_{in} =$ initial (nonequilibrium) ratio of k_{forw}/k_{rev}. This value was found by applying least-squares regression to the lab scale packed-bed reactor data. A value of $K_{in} = 12.7$ minimized the error between the observed data and the concentrations predicted by the model. After the first iteration, the value of EDB_{surf} was calculated using Eq. (11).

The concentration of EDB on the reactive surface was dependent on mass transfer and the surface reaction. The rate of surface reaction was calculated using E_a and A from the batch experiments

$$k_1 = A \exp\left(\frac{E_a}{RT}\right) \quad (10)$$

Combining the mass transfer terms and the surface reaction term gave the rate of change of $[EDB_{surf}]$.

$$\frac{d[EDB_{surf}]}{dt} = k_{forw}a[EDB_{aq}] - k_{rev}[EDB_{surf}] - k_1a[EDB_{surf}] \quad (11)$$

k_{forw} came from Eq. (7). Eq. (10) gave the value for k_1, and $k_{rev} = k_{forw}/K_{ads}$. The fit of the lab scale data was found to be independent of k_1 indicating that mass transfer controlled the removal rate of EDB in the lab scale experiments.

Pilot Scale Packed-Bed Reactor

After a brief period of in-house testing, the pilot scale system was transported to MMR in October 1998. The pilot plant was in use for 8 months from October 1998 to June 1999, more than 82,000 L of groundwater were treated. The EDB influent concentration declined throughout the length of the experiment due to ongoing treatment of the plume, $[EDB]_0 = 7-3$ ppb. Dissolved oxygen was removed from the influent ($DO < 0.5$ mg/L) in the first canister. The pH increased from initial values of 6.8 ± 0.5 to a steady value of 7.3 ± 0.5 after the first canister and remained relatively constant throughout the system at all flow rates.

Three influent flow rates were used; 300, 600, and 2,000 mL/min. Many pore volumes (100–400) were required for the concentrations to reach steady state. The number of pore volumes required depended on flow rate and the concentration of EDB. Sorption to nonreactive surfaces has been shown to cause the retardation of solutes in porous media, however, once steady state conditions are reached, nonreactive sorption will not affect the extent of reaction (Hatfield et al. 1996).

Fig. 7 shows EDB concentrations in the pilot system for a flow of 600 mL/min. The data from 37 to 645 pore volumes shows the delay in reaching steady state conditions. Once steady state was reached the EDB profile through the pilot plant was stable for hundreds of pore volumes. The target effluent concentration of $[EDB] = 0.02$ ppb was not reached. The removal efficiencies for
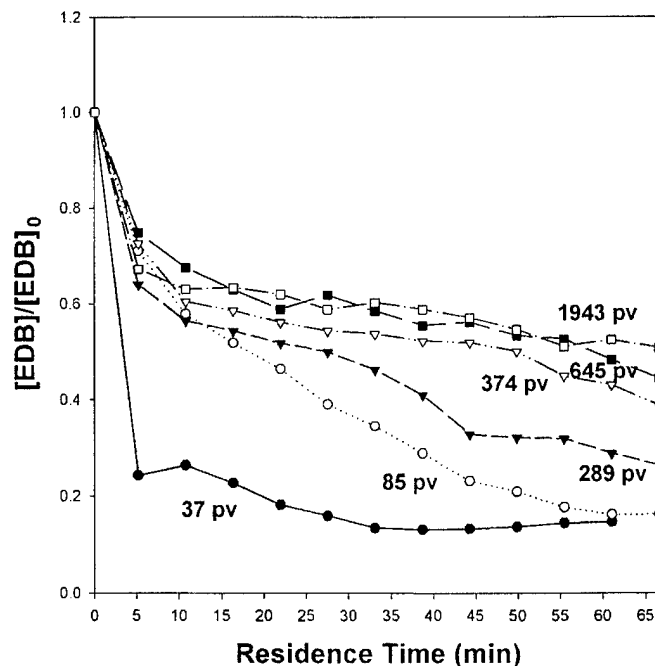

Fig. 7. Ethylene dibromide (EDB) concentration profile through the pilot plant, $V = 600$ mL/min. The concentrations at each sample point increase over time (from 37 to 1943 pore volumes) until steady state conditions are reached. Once steady state is reached the profile is stable for hundreds of pore volumes, 645–1943 pore volumes. The initial rapid drop is due to nonequilibrium mass transfer. The removal of EDB from canisters 2–12 is dominated by the rate of the surface reaction.

flows of 300 mL/min, 600, and 2,000 after the last canister (12), were 73, 49, and 39% respectively.

The concentration profile through the pilot plant showed two regions. The first was a sharp reduction in EDB concentration after the first canister (at 300 mL/min, after the second canister). After that, the EDB concentrations declined slowly and steadily. Pseudo-first-order rate constants for EDB removal in these two regions show that in the first the rate constants (k_{first}) increased with increasing flow rate. In the second region the rate constants (k_{sec}) were independent of flow rate (Table 2 and Fig. 7).

This dependence on linear velocity in the first region was similar to that observed in the lab scale studies. This showed that mass transfer dominated in the early stages of the pilot scale reactor but once the transient nonequilibrium conditions had passed the rate of surface reaction controlled the kinetics.

The data from the pilot scale experiments were simulated using the model developed from the batch isotherm and the mass transfer equations from the lab scale studies. The pilot scale system had a different reactor configuration (Table 1), lower process temperatures, and lower initial EDB concentrations than those

Table 2. Pseudo-First-Order Rate Constants From Pilot Plant Experiments

Flow rate (L/min)	V (cm/min)	N_{Re}	k_{first} (min^{-1})	k_{sec} (min^{-1})
0.3	4.8	0.42	$0.052 \pm .004$	$0.014 \pm .004$
0.6	9.6	0.84	$0.138 \pm .048$	$0.013 \pm .005$
2.0	32.2	2.79	$0.249 \pm .086$	$0.019 \pm .012$

Note: k_{first} rate constants were calculated using the first three data points (influent to canister 2). k_{sec} constants were derived from the steady state ethylene dibromide concentrations in canisters 2–12.
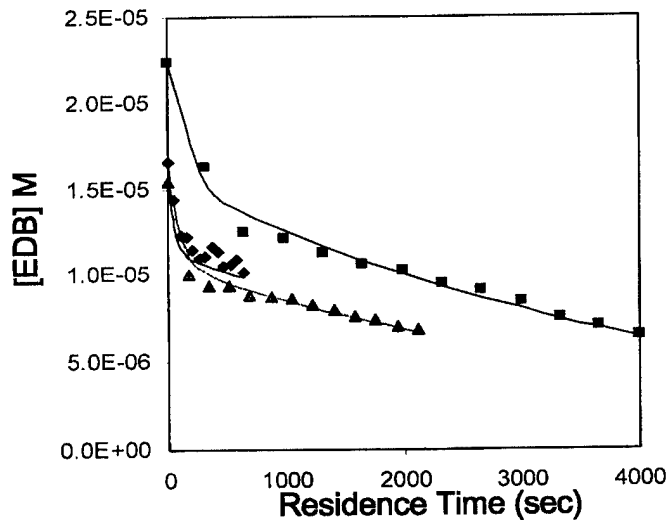
Fig. 8. Pilot scale packed-bed reactor data and model simulations. $V=300$ mL/min (data ■, model —), $[EDB]_0=22.3$ μM, $T=11.0°C$, $r^2=0.99$; $V=600$ mL/min (data ▲, model —), $[EDB]_0=15.4$ μM, $T=11.3°C$, $r^2=0.98$; $V=2,000$ mL/min (data ◆, model —), $[EDB]_0=15.4$ μM, $T=12.2°C$, $r^2=0.93$.

used in the lab scale experiments. Variables such as $[EDB]_0$, temperature, and flow rate were entered into the model as initial parameters. The K_{in} value was fitted by the least squares method using data from all three flow rates and was determined to be 22 (m^3/m^2). Fig. 8 shows the experimental data and the model predictions of three data sets (flow=300, 600, and 2,000 mL/min). The correlation between data and model were strong ($r^2 > 0.93$). The model was able to predict the two regions in the EDB profile that were seen in the pilot plant data.

The model was used to design a hypothetical above ground treatment system for conditions similar to FS-12 MMR. The system was scaled up by keeping N_{Re} and the reactor length/cross sectional area ratio (L/A) within an order of magnitude of those of the lab and pilot scale reactors (Table 1). Using the current influent conditions of FS-12 MMR, $[EDB]_0=3$ ppb, and flow rate=612 gal/min (2.3 m^3/s), a packed-bed reactor with a cross sectional area of 3.0 m, a length of 110 m, and a hydraulic retention time of 3.1 hours would be required to reach an effluent EDB concentration less than 20 ppt.

A hypothetical hydraulic fracture placement PRB was also modeled. The average groundwater flow rate at FS-12 MMR is 1.5 ft/day (5.3 μ/s) (MMR 2000). Hocking et al. (1998) reported that the average thickness of a PRB emplaced by hydraulic fracture was 0.089 m (3.5 in.). Assuming a groundwater temperature of 11°C, and that ε and a were the same as the packed-bed reactor, an initial EDB concentration of 3 ppb, a wall thickness of 0.164 m (6.5 in.) would be required to achieve the EDB MCL level of 20 ppt.

Conclusions

Mass transfer and sorption played significant roles in the kinetics of EDB removal by cast iron packed-bed reactors. Initially there was significant nonreactive sorption of EDB to the iron surface (Fig. 7). Tens of pore volumes were required to reach partitioning equilibrium.

Lab scale column studies varying flow rates and initial EDB concentrations exhibited characteristics of nonequilibrium sorption. Observed removal rates of EDB in aqueous solutions increased at higher flow rates. Increasing $[EDB]_0$ decreased the apparent removal rates (Fig. 5). Modeling of the system indicated that under nonequilibrium conditions there was rapid sorption to surface sites, at higher $[EDB]_0$ and longer retention times (lower V), this phenomenon diminished.

The pilot plant experiments were run for several months at three flow rates. The longer hydraulic retention times in the pilot plant relative to the bench scale columns revealed that after the transitory nonequilibrium conditions removal was dominated by the rate of the surface reaction. These transitory conditions complicated the analysis of the system kinetics. Studies done with short columns over predicted removal rates and would have lead to under sizing of packed-bed reactors.

Packed-bed ZVI reactors may provide an alternative to the current best available technology, granular activated carbon (GAC). The advantages of ZVI included the detoxification of EDB and lower operation and maintenance costs the GAC. Packed-bed ZVI reactors may be useful treatment options for pump-and-treat remediation of EDB contaminated groundwaters. Jetting or hydraulic fracture placement of ZVI PRB may also provide in situ treatment options for EDB contaminated groundwater.

Acknowledgments

Notation

The following symbols were used in this paper:

A = cross-sectional area of reactor (m^2);
A = Arrhenius parameter;
a = iron surface area/liquid volume (m^2/m^3);
C = mass transfer constant;
C_{surf} = concentration of sorbed solute (mol/m^2);
D_{EDB} = diffusivity of EDB in water (m/s);
d_p = particle average cross sectional diameter (m);
E_a = activation energy, kJ/mol;
EDB_{max} = maximum concentration of surface sites (mol/m^2);
EDB_{surf} = concentration of sorbed EDB (mol/m^2);
f = flow rate (m^3/s);
K_{ads} = equilibrium constant (m^3/m^2);
K_{in} = initial ratio of k_{forw}/k_{rev};
k_{first} = observed rate constant of EDB removal in first region (min^{-1});
k_{forw} = sorption rate constant (s^{-1});
k_{mt} = general mass transfer rate constant (m^3/m^2s);
k_{obs} = observed removal rate constant of lab scale experiments (s^{-1});
k_{rev} = desorption rate constant (s^{-1});
k_{sec} = observed rate constant of EDB removal in second region (min^{-1});
k_1 = rate constant of surface reaction (m^3/m^2s);
L = reactor length (m);

N_{Re} = particle Reynolds number;
S = Reynolds number exponent;
S_{sat} = $[EDB_{surf}]$ at equilibrium (mol/m^2);
Sc = Schmidt number;
V = linear velocity (m/s);
ε = porosity; and
η = kinematic viscosity of water (m^2/s).

References

Agrawal, A., and Tratnyek, P. (1996). "Reduction of nitro aromatic compounds by zero-valent iron metal." *Environ. Sci. Technol.*, 30, 153–160.

Arnold, W. A., Ball, W. P., and Roberts, A. L. (1999). "Polychlorinated Ethane Reaction with Zero-Valent Zinc: Pathways and Rate Control." *J. Contam. Hydrol.*, 40, 183–200.

Baciocchi, E. (1983). "Chapter 5: The chemistry of functional groups supplement D." *1,2-Dehalogenations and related reactions*, Patai, S., and Rappoport, Z., eds., Wiley, New York.

Burris, D., Allen-King, R., Manoranjan, V., Campbell, T., Loraine, G., and Deng, B. (1998). "Chlorinated ethene reduction by cast iron: Sorption and mass transfer." *J. Environ. Eng.*, 124(10), 1012–1019.

Campbell, T., Burris, D., Roberts, A. L., and Wells, J. R. (1997). "Trichloroethylene and tetrachloroethylene reduction in a metallic iron-water-vapor batch system." *Envir. Toxicol. Chem.*, 16(4), 625–630.

Carberry, J. J. (1976). *Chemical and catalytic reaction engineering.* McGraw-Hill, New York.

Fetter, C. W. (1993). *Contaminant hydrogeology*, Macmillan, New York.

Gavasker, A., Sass, B., Gupta, N., Hicks, J., Yoon, S., Fox, T., and Sminchak, J. (1999). "Cost and performance report for the performance evaluation of a pilot-scale permeable barrier at former naval air station moffet field, Mountain View, Calif." *Contract Rep. CR 99 003-ENV*, Naval Facilities Engineering Service Center, Calif.

Gillhiam, R., and O'Hannesin, S. (1994). "Enhanced degradation of halogenated aliphatics by zero-valent iron." *Ground Water*, 32(60), 958–967.

Hatfield, K., Burris, D., and Wolfe, N. (1996). "Analytical model for heterogeneous reactions in mixed porous media." *J. Environ. Eng.*, 122(8), 676–684.

Hocking, G., Wells, S. L., and Ospina, R. I. (1998). "Field performance of vertical hydraulic fracture placed iron reactive walls." *Proc., Designing and applying treatment technologies; remediation of chlorinated and recalcitrant compounds, 1st Int. Conf. remediation of chlorinated and recalcitrant compounds*, Battelle, Monterey, Calif., 151–156.

Hundal, L., Singh, J., Bier, E., Shea, P., Comfort, S., and Powers, W. (1997). "Removal of TNT and RDX from Water and Soil Using Iron Metal." *Environ. Pollut.*, 97(1–2), 55–64.

Johnson, T., Scherer, M., and Tratnyek, P. (1996). "Kinetics of halogenated organic compound degradation by iron metal." *Environ. Sci. Technol.*, 30, 2634–2640.

Matheson, L., and Tratnyek, P. (1994). "Reductive dehalogenation of chlorinated methanes by iron metal." *Environ. Sci. Technol.*, 28, 2045–2053.

"MMR base history." (2000). http://www.mmr.org/mmr1/bashist.htm (Mar. 9, 2000).

O'Hannesin, S., and Gillham, R. (1998). "Long-term performance of an in-situ "iron wall" for remediation of VOC's." *Ground Water*, 36(1), 164–170.

Puls, R., Blowes, D., and Gillham, R. (1998). "Emplacement verification and long-term performance monitoring for permeable reactive barrier at the USCG Support Center, Elizabeth City, North Carolina." *U.S. EPA, Rep. No. EPA 600/A-98-085*, Washington, D.C.

Rajagopal, V., and Burris, D. (1999). "Reduction of 1,2-dibromoethane in the presence of zero-valent iron." *Envir. Toxicol. Chem.*, 18(8), 1779–1782.

Sanders, R. (1999). "Compilation of Henry's law constants for inorganic and organic species of potential importance in environmental chemistry." www.mpch-mainz.mpg.de/~sanders/res/henry.html (April 8, 1999).

Sayles, G., You, G., Wang, M., and Kupferle, M. (1997). "DDT, DDD, and DDE dechlorination by zero-valent iron." *Environ. Sci. Technol.*, 31, 3448–3454.

Shokes, T., and Moller, G. (1999). "Removal of dissolved heavy metals from acid rock drainage using iron metal." *Environ. Sci. Technol.*, 33, 282–287.

Siantar, D., Schreier, C., Chou, C.-S., and Reinhard, M. (1996). "Treatment of 1,2-dibromo-3-chloropropane and nitrate-contaminated water with zero-valent iron or hydrogen/palladium catalysts." *Water Resour.*, 30(10), 2315–2322.

Wilson, E. J., and Geankopolis, C. J. (1964). "Liquid mass transfer at very low Reynolds numbers in packed beds." *Ind. Eng. Chem. Fundam.*, 5(1), 9–14.